1-1-2012

Degradation of dc characteristics of InAlN/GaN high electron mobility transistors by 5 MeV proton irradiation

Chien-Fong Lo

L. Liu

T. S. Kang

Fan Ren

C. Schwarz
University of Central Florida

See next page for additional authors

Degradation of dc characteristics of InAlN/GaN high electron mobility transistors by 5 MeV proton irradiation

Chien-Fong Lo, L. Liu, T. S. Kang, Fan Ren, C. Schwarz, E. Flitsiyan, L. Chernyak, Hong-Yeol Kim, Jihyun Kim, Sang Pil Yun, O. Laboutin, Y. Cao, J. W. Johnson, and S. J. Pearton

Citation: Journal of Vacuum Science & Technology B **30**, 031202 (2012); doi: 10.1116/1.3698402
View online: https://doi.org/10.1116/1.3698402
View Table of Contents: https://avs.scitation.org/toc/jvb/30/3
Published by the American Vacuum Society

Degradation of dc characteristics of InAlN/GaN high electron mobility transistors by 5 MeV proton irradiation

Chien-Fong Lo, L. Liu, T. S. Kang, and Fan Ren
Department of Chemical Engineering, University of Florida, Florida 32611, Gainesville

C. Schwarz, E. Flitsiyan, and L. Chernyak
Physics Department, University of Central Florida, Florida 32816, Orlando

Hong-Yeol Kim and Jihyun Kim
Department of Chemical & Biological Engineering, Korea University, Anam-dong, Sungbuk-gu, Seoul, Korea

Sang Pil Yun
Korea Atomic Energy Research Institute, 1045 Daedeok Street, Yuseong-gu, Daejeon, Korea

O. Laboutin, Y. Cao, and J. W. Johnson
Kopin Corporation, Taunton, Massachusetts 02780

S. J. Pearton[a)]
Department of Materials Science and Engineering, University of Florida, Gainesville, Florida

(Received 9 January 2012; accepted 12 March 2012; published 27 March 2012)

The dc characteristics of InAlN/GaN high electron mobility transistors were measured before and after irradiation with 5 MeV protons at doses up to 2×10^{15} cm^{-2}. The on/off ratio degraded by two orders of magnitude for the highest dose, while the subthreshold slope increased from 77 to 122 mV/decade under these conditions. There was little change in transconductance or gate or drain currents for doses up to 2×10^{13} cm^{-2}, but for the highest dose the drain current and transconductance decreased by ~40% while the reverse gate current increased by a factor of ~6. The minority carrier diffusion length was around 1 μm independent of proton dose. The InAlN/GaN heterostructure is at least as radiation hard as its AlGaN/GaN counterpart. © *2012 American Vacuum Society*. [http://dx.doi.org/10.1116/1.3698402]

I. INTRODUCTION

GaN–based heterostructures are radiation hard materials for which much basic information on the effects of radiation on charge collection, stoichiometric disturbances, defect creation, and the scaling of these effects at small volumes is missing. There are three main GaN-based heterostructures used for electronics, namely,[1–3] (i) AlGaN/GaN, which is the most common nitride-based heterostructure, (ii) AlN/GaN, which produces the highest two dimensional electron gas density, but has issues with stability of the AlN, and (iii) InAlN/GaN, an emerging system with high thermal and chemical stability and lattice matching to GaN at an In mole fraction of 0.17.[2,3]

Previous studies indicate the AlGaN/GaN heterostructure exhibits radiation tolerances up to two orders of magnitude higher than the GaAs/AlGaAs system, based on the higher bond strengths and displacement energies in the nitrides.[4–14] We have reported changes of ~30% in transconductance in AlGaN/GaN heterostructures exposed to high energy 40 MeV protons at doses of 5×10^{10} cm^{-2}, equivalent to a decade in low earth-orbit.[4,8,9] The carrier removal rate for proton irradiated n-GaN was found to be around 10^2–10^3 cm^{-1}, depending on the proton energy and was shown to increase for higher donor concentrations.[5]

The most prominent defects created by protons are deep traps due to N vacancies with ionization energy of 0.07 eV[5]. Other traps are tentatively ascribed to Ga vacancy complexes with nitrogen interstitials. These defects can be annealed at low temperatures of ~300 °C. For high doses of proton or heavier ions, aggregates of primary defects can be formed, with activation energies of 0.75 and 0.95 eV. Comparison of defect production efficiency for 2 MeV protons and 2.5 MeV electrons showed that the protons were 1000 times more effective, whereas calculations of the number of displaced atoms based on the measured threshold energy predicted the ratio of 250. The discrepancy was attributed to the difference in defects self-annealing rates depending on irradiating particle type and energy.[5]

The InAlN/GaN material system offers an attractive alternative to AlGaN/GaN for high power, high frequency applications.[15,16] The InAlN alloy can be synthesized lattice matched to GaN with large refractive index contrast and sheet charge density roughly twice that of typical AlGaN/GaN HEMTs. This sheet charge density is due to the more than 4× increase in spontaneous polarization of $In_{0.17}Al_{0.83}N$/GaN as compared to a traditional $Al_{0.2}Ga_{0.8}N$/GaN HEMT. Although there is no strain-induced piezoelectric component to the overall polarization charge of the lattice-matched InAlN heterostructures, the spontaneous component dominates and leads to a total polarization charge more than 2× that of $Al_{0.2}Ga_{0.8}N$/GaN. This enables extremely high sheet charge density even in thin (~10 nm) barrier HEMT structures. These properties can be exploited to fabricate InAlN/GaN HEMTs with very high current density, low access resistance, aggressive scaling, and

a)Electronic mail: spear@mse.ufl.edu

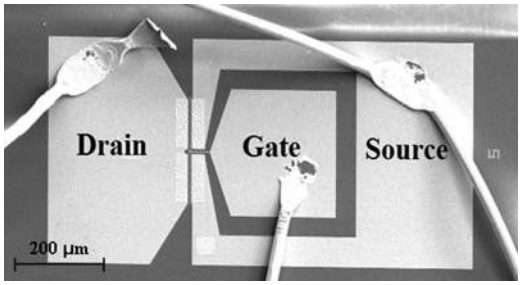

FIG. 1. Optical micrograph of InAlN/GaN HEMT device layout.

monolithic integration of normally-on and normally-off operation.[2,3]

Little is known about the effects of radiation on the InAlN/GaN heterostructure, especially since it has lower defect density and an absence of lattice-mismatch induced strain compared to the more common AlGaN/GaN system.[15] In this paper we report on the degradation of dc characteristics of InAlN/GaN high electron mobility transistors (HEMTs) exposed to different doses of 5 MeV protons.

II. EXPERIMENT

The HEMTs were grown by metal organic chemical vapor deposition, starting with a thin AlGaN nucleation layer, followed by a 1.9 μm C-doped GaN buffer layer, 50 nm undoped GaN layer, 10 nm undoped InAlN layer with 17% indium mole fraction, and capped with 2.5 nm undoped GaN layer.[16] The growth was on 3 in. diameter SiC substrates. Hall measurements showed sheet carrier densities of 2×10^{13} cm^{-2} and electron mobility of 1000 cm^2/V s. Device fabrication involved Ohmic contact deposition with standard lift-off e-beam evaporated Ti/Al/Ni/Au annealed at 800 °C for 30 s under N_2 ambient. Multiple energy and dose nitrogen implantation were used for device isolation and AZ1045 resist used as the mask to define the active region of the devices. Isolation currents were <10 nA at 40 V bias across two 100 μm × 100 μm Ohmic pads separated by a 5 μm implanted gap. 1 μm gates were defined by lift-off of an e-beam evaporated metal stack of Pt/Ti/Au. Ti/Au metallization was used for the interconnect metals for source, gate, and drain electrodes. The transistors were passivated with 400 nm of plasma enhanced chemical vapor deposited SiN_x at 300 °C, followed by opening of contact windows using plasma etching. dc I-V characteristics were measured with Agilent. The projected range of the protons is >50 μm from the stopping of ions in matter simulation code that is standard in ion stopping experiments. Measurements were taken ~50 h after irradiation.

TABLE I. Summary of ideality factor and Schottky barrier height of InAlN/GaN HEMTs before and after proton irradiations with different proton doses.

Proton dose	Preirradiation	2×10^{11} cm^{-2}	2×10^{13} cm^{-2}	2×10^{15} cm^{-2}
Ideality factor	1.8	1.6	1.5	1.3
Schottky barrier height (V)	0.83	0.85	0.88	0.89

Proton irradiations were performed at the Korean Institute of Radiological & Medical Sciences (KIRAMS) using a cyclotron. The proton energy at the exit of the cyclotron was 30 MeV. The proton energy at the sample was 5 MeV after passing through two aluminum degraders[15]. The thickness of each aluminum degrader was 2.7 mm. The beam currents were measured using Faraday-cup to calculate flux density. The proton dose was varied from 2×10^{11} to 2×10^{15} cm^{-2}.

Current-voltage (I-V) characteristics were measured for the HEMTs before and after the proton irradiation, including transconductance (g_m) and subthreshold characteristics at various doses using an Agilent 4155C. Electron beam induced current (EBIC) measurements were conducted *in situ* in a SEM and under an electron beam accelerating voltage of 20 kV. Measurements were taken between the gate and the drain at 25 000× magnification. A diffusion length was calculated from the EBIC measurements for each sample at temperatures varying from 25–125 °C. Figure 1 shows an optical micrograph of a bonded device used for these measurements.

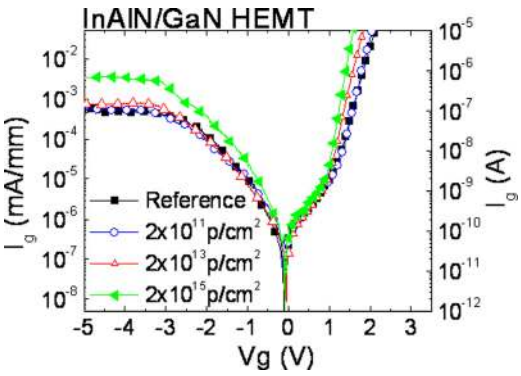

FIG. 2. (Color online) Gate I-V characteristics before and after proton irradiation with different doses.

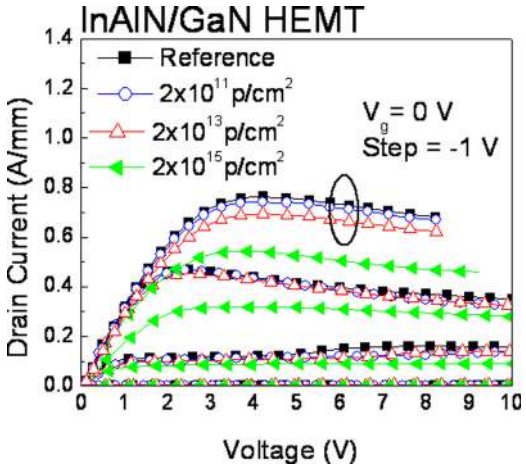

FIG. 3. (Color online) Drain I-V characteristics before and after proton irradiation with different doses. The gate voltage was stepped from 0 V in − 1 V steps.

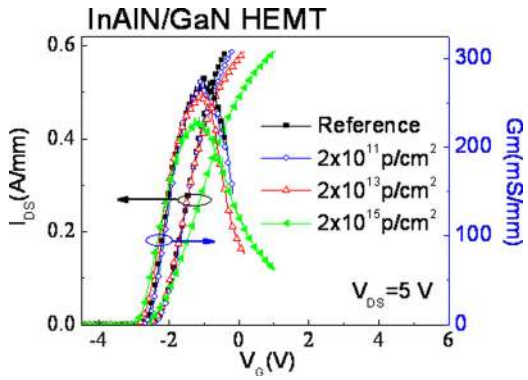

FIG. 4. (Color online) Transfer characteristics before and after proton irradiation with different doses. The drain-source voltage was 5 V.

III. RESULTS AND DISCUSSION

Figure 2 shows the gate I-V characteristics from the InAlN/GaN HEMTs before and after proton irradiation with different doses. There was little change in either forward or reverse gate currents up to doses of 2×10^{13} cm^{-2}, while at the highest dose of 2×10^{15} cm^{-2} the reverse current was increased by about a factor of 6. Table I summarizes the changes in Schottky barrier height and diode ideality factor as a result of the different proton doses. While there are modest changes in both parameters with increasing dose, the effect of the defect introduction by the proton irradiation dominates and leads to the observed increases in gate current.

Figure 3 shows the corresponding drain I-V characteristics before and after proton irradiation with different doses. Once again, there was little change for doses up to 2×10^{13} cm^{-2}, but for the highest dose the drain current decreased by ~40%. We expect this is due to the introduction of deep electron traps in the InAlN and GaN channel layers that remove electrons from the conduction process. Similar trends were observed for the HEMT transconductance, as shown in the transfer characteristics of Fig. 4. Note that this highest dose of 2×10^{15} cm^{-2} corresponds to the proton flux encountered in roughly 4×10^5 yr in low earth orbit. We did not observe any degradation in the contact metallurgy for this dose.

Figure 5 shows the changes in subthreshold drain I-V curves after proton irradiation with different doses and the resulting changes in subthreshold slope are summarized in Table II, along with the degradation in on/off ratio. The on/off ratio degraded by two orders of magnitude for the highest dose, while the subthreshold slope increased from 77 to 122 mV/decade under these conditions. These changes are consistent with an increase in channel resistance and an increase in gate current due to creation of deep electron traps. Note that the changes in dc characteristics of the HEMTs are generally on the lower side of those observed for AlGaN/GaN HEMTs, showing that the InAlN/GaN heterostructure is at least as radiation hard as its more common counterpart.

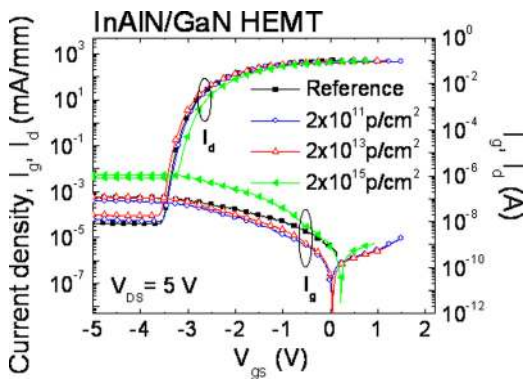

FIG. 5. (Color online) Subthreshold drain I-V curves after proton irradiation with different doses. The drain-source voltage was 5 V.

TABLE II. Summary of subthreshold slope, ON/OFF ratio, sheet and transfer resistance and minority carrier diffusion length of InAlN/GaN HEMTs before and after proton irradiations with different proton doses.

Proton doses	Preirradiation	2×10^{11} cm^{-2}	2×10^{13} cm^{-2}	2×10^{15} cm^{-2}
Subthreshold slope (mV/dec)	77	83	92	122
ON/OFF ratio	1.2×10^7	8.1×10^6	4.9×10^6	1.1×10^5
Diffusion length	0.98	1.03	1.07	1.09
Transfer resistance (Ohm mm)	0.65	0.86	0.95	1.21
Sheet resistance (Ohms per square)	292	315	326	469
Threshold voltage shift (V)	0	0	0.1	0.6

Figure 6(a) shows a scanning electron microscope (SEM) image indicating where the EBIC measurements were taken, while Fig. 6(b) shows SEM images with EBIC signal as a function of distance. Figure 7 shows the EBIC signal (V) vs distance (μm) for the reference and three irradiated samples offset for clarity. If the incident electron beam is perpendicular to a planar Schottky barrier, created on the material's top

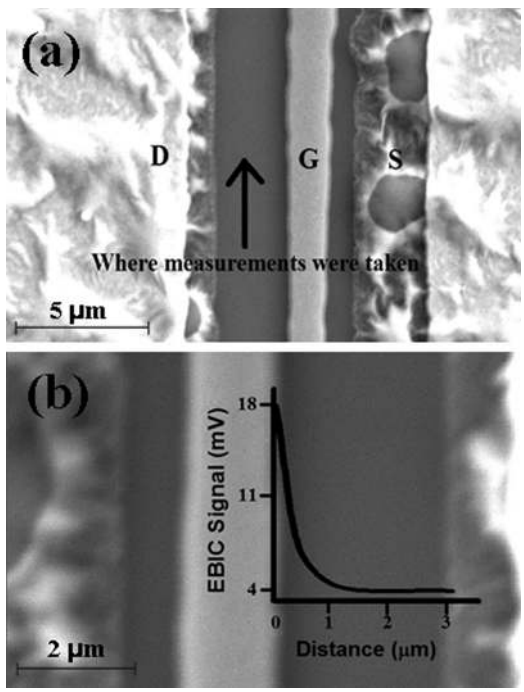

FIG. 6. (a) SEM Image indicating where the EBIC measurements were taken. (b) SEM images with EBIC signal vs distance.

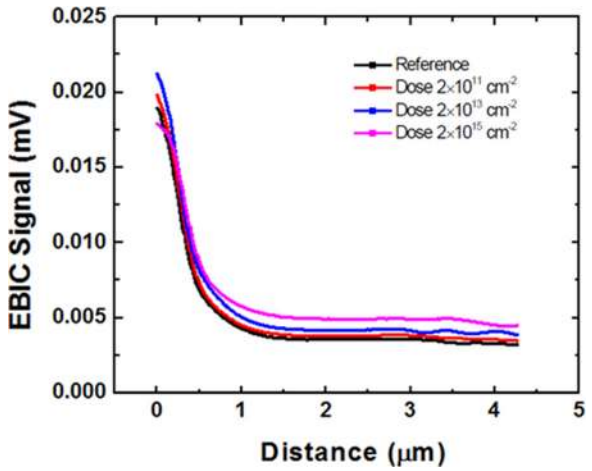

FIG. 7. (Color online) EBIC signal (V) vs distance (μm) for the reference and three irradiated samples off set for clarity.

surface, the EBIC signal, I, decays with the beam-to-barrier distance, d, according to the relationship[17–19]

$$I = Ad^{\alpha}\exp(-d/L). \quad (1)$$

Here A is a constant, L is the diffusion length, and α is a coefficient that depends on the surface recombination velocity, v_s. This coefficient varies from $\alpha = -1/2$, for $v_s = 0$, to $\alpha = -3/2$, for infinite v_s. Since infinite surface recombination velocity is very unlikely in view of the excellent luminescence efficiency of GaN, the value of $\alpha = -1/2$ was used in this work. Equation (1) yields a straight line relationship for a plot of $\ln(I \times d^{1/2})$ versus d. The diffusion length L can be then obtained directly as -1/slope. The minority carrier diffusion length was close to 1 μm independent of proton dose, showing that even at the highest value, the material transport remains quite good and the crystal structure is not amorphized.

IV. SUMMARY AND CONCLUSIONS

InAlN/GaN HEMTs were irradiated with 5 MeV protons to doses of 2×10^{15} cm^{-2}. The changes in device dc characteristics were modest to doses of 2×10^{13} cm^{-2} and even at the highest dose the drain current and transconductance decreased by ~40% while the reverse gate current increased by a factor of ~6. The on/off ratio degraded by two orders of magnitude under these conditions. The InAlN/GaN system looks promising for space-borne applications where high proton fluxes can be expected.

ACKNOWLEDGMENTS

The work at UF is supported by an AFOSR MURI monitored by Jim Hwang and by HDTRA (Don Silversmith) under Contract U.S. DOD HDTRA, Grant No. 1-11-1-0020. The work at UCF is supported by NSF (ECCS #0900971) and Israel Ministry of Defense (Contract #4440341314).

[1]C. Y. Chang, S. J. Pearton, C. F. Lo, F. Ren, and A. M. Dabiran, Appl. Phys. Lett. **94**, 263505 (2009).
[2]J. Kuzmik, A. Kostopoulos, G. Konstantinidis, J.-F. Carlin, A. Georgakilas, and D. Pogany, IEEE Trans. Electron Dev. **53**, 422 (2006).
[3]J. W. Chung, O. I. Saadat, J. M. Tirado, X. Gao, S. Guo, and T. Palacios, IEEE Electron. Device Lett. **30**, 904 (2009).
[4]B. Luo, J. W. Johnson, F. Ren, S. J. Pearton, and A. M. Dabiran, Appl. Phys. Lett. **79**, 2196 (2001).
[5]S. J. Pearton and A. Y Polyakov, Int. J. Mater. Struct. Integr. **2**, 93 (2008).
[6]F. Gaudreau and A. Houdayer, IEEE Trans. Nucl. Sci. **49**, 2702 (2002).
[7]B. D. White, D. M. Fleetwood, and R. D. Schrimpf, IEEE Trans. Nucl. Sci. **50**, 1934 (2003).
[8]B. Luo, J. W. Johnson, F. Ren, S. J. Pearton, and A. M. Dabiran, Appl. Phys. Lett. **79,** 2196 (2001).
[9]B. Luo, F. Ren, S. J. Pearton, A. Dabiran, P. P. Chow, and A. G. Baca, J. Electron. Mater. **31**, 437 (2002).
[10]J. Kim, B. P. Gila, R. Mehandru, F. Ren, and S. J. Pearton, Electrochem. Solid State **5**, G57 (2002).
[11]B. Luo, F. Ren, and S. J. Pearton, Electrochem. Solid State **6**, G31 (2003).
[12]B. Luo, F. Ren, K. Allums, and S. J. Pearton, Solid-State Electron. **47**, 1015 (2003).
[13]K. K. Allums, S. J. Pearton, and F. Ren, J. Electron. Mater. **36**, 519 (2007).
[14]J. Kim, F. Ren, and S. J. Pearton, J. Electrochem. Soc. **155**, H513 (2008).
[15]C. Lo *et al.*, J. Vac. Sci. Technol. B **29**, 061201 (2011).
[16]C. F. Lo *et al.*, J. Vac. Sci. Technol. B **29**, 021002 (2011).
[17]D. S. H. Chan, V. K. S. Ong, and J. C. H. Phang, IEEE Trans. Electron. Devices **42**, 963 (1995).
[18]H. J. Leamy, J. Appl. Phys. **53**, R51 (1982).
[19]O. Lopatiuk-Tirpak, L. Chernyak, Y. L. Wang, F. Ren, S. J. Pearton, K. Gartsman, and Y. Feldman, Appl. Phys. Lett. **90**, 172111 (2007).